PHYSICAL REVIEW B VOLUME 4, NUMBER 6 15 SEPTEMBER 1971

Lattice Dynamics of fcc Argon with Three-Body Forces*

M. L. Klein
Division of Chemistry, National Research Council of Canada, Ottawa, Canada

and

J. A. Barker and T. R. Koehler
IBM Research Laboratory, San Jose, California 95114

(Received 9 April 1971)

Phonon spectra are calculated for fcc ^{36}Ar at 4, 40, and 77 °K using the pair potential for argon atoms derived by Bobetic and Barker. The calculation employs a quasiharmonic basis with three-body forces and a perturbation-theory treatment of the anharmonicity. Poor agreement is obtained with the experimental temperature shifts of transverse phonons propagating along the [ξ00] direction. Self-consistent phonons are also calculated at 0 °K for both the Bobetic-Barker and Dymond-Alder potentials. On the basis of existing phonon data, the latter appears to be ruled out as a realistic pair potential.

I. INTRODUCTION

There has been considerable interest in the lattice dynamics of rare-gas solids and much speculation on the possible role of nonpairwise additivity of the interatomic forces.[1,2] From analysis of low-density gas-phase properties, Barker and Pompe[3] proposed the following pair potential $\phi^{(2)}(ij)$ for two Ar atoms separated by a distance R_{ij}:

$$\phi^{(2)}(R)=\epsilon\left[e^{\alpha(1-R)}\sum_{n=0}^{L}A_n(R-1)^n-\sum_{n=0}^{2}\left(\frac{C_{2n+6}}{\delta+R^{2n+6}}\right)\right], \quad (1)$$

where $R=R_{ij}/R_m$, with R_m and ϵ being the separation and depth at the minimum of the potential. Potentials of the form given by Eq. (1) were found to fit well all available two-body gas data. However, the third virial coefficient derived from these same potentials was incompatible with experiments indicating the presence of an explicit three-body force. Barker and Pompe found[3] that the third virial coefficient could be fitted by including the Axilrod-Teller triple-dipole force[4]

$$\phi^{(3)}(ijk)=\nu(1+3\cos\theta_1\cos\theta_2\cos\theta_3)/(R_1R_2R_3)^3\,, \quad (2)$$

where θ_1, θ_2, θ_3, and R_1, R_2, R_3 are the interior angles and sides of the triangle formed by the three atoms and ν is calculated from known oscillator strengths and sum rules of the atomic absorption spectrum. If the total potential energy Φ of N Ar atoms were written

$$\Phi=\sum_{i>j}\phi^{(2)}(ij)+\sum_{i>j>k}\phi^{(3)}(ijk)\,, \quad (3)$$

with $\phi^{(2)}(ij)$ and $\phi^{(3)}(ijk)$ taken from Eqs. (1) and (2), liquid properties were also well fitted.[5] A small refinement of the Barker-Pompe potential (see Fig. 1) by Bobetic and Barker[1] enabled many of the low-temperature thermodynamic properties of solid Ar to be fit also. In addition the calculated phonon dispersion curves at 4 °K were in excellent agreement with experiment.[2] All these facts taken together suggest that Eqs. (1)–(3) provide a good representation of the forces in solid Ar.

Various other potentials have been proposed for Ar. Dymond and Alder,[6] for example, obtained a numerical potential function $\phi^{(2)}(ij)$ from gas-phase data which fitted the two-body data as well as either the Bobetic-Barker or Barker-Pompe potentials.[7] Qualitatively the Dymond-Alder potential was similar to that of Bobetic and Barker but in detail it had a much wider potential bowl,[1] implying a very anharmonic potential. Unfortunately, this pair potential is not in agreement with recent spectroscopic studies of the Ar_2 molecule[8] and we shall see that it is also in poor agreement with the phonon spectrum of the solid.

The object of the present paper is the detailed calculation of phonon spectrum of solid argon as a function of temperature using the potentials described above. The study is motivated by the recent measurement of the temperature dependence of the transverse phonon branch for the [ξ 0 0] direction in fcc ^{36}Ar by Batchelder, Saunderson, and Haywood.[9] These new data, which are the first in rare-gas solids to extend close to melting, should provide a rather stringent test of both the interatomic forces and the lattice dynamical model.

The outline of the paper is as follows. In Sec. II we present the pertinent theory and give detailed results for the Bobetic-Barker potential, including three-body forces and a perturbation theory of the anharmonic effects using a quasiharmonic basis. This procedure should be adequate up to about

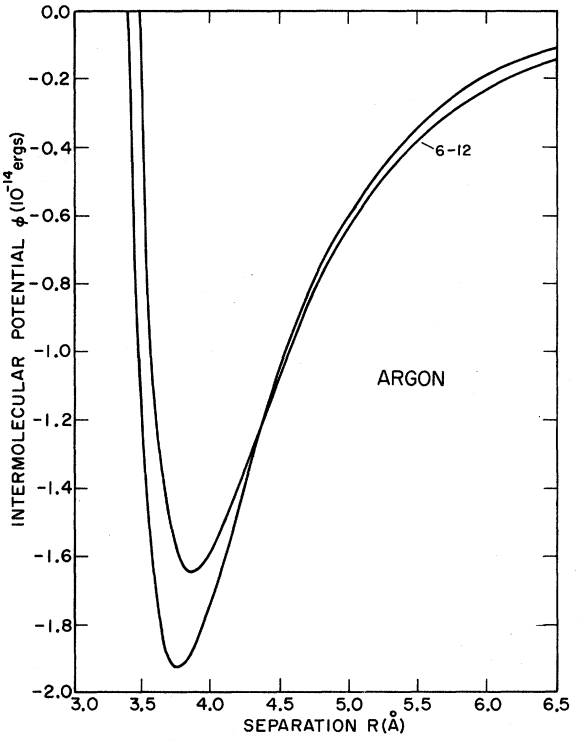

FIG. 1. Interatomic potentials for two Ar atoms. The curve (6-12) is the familiar Lennard-Jones potential taken from Ref. 18. The other curve is the Bobetic-Barker potential as described in the text.

one-half the melting temperature, provided that the lattice constant is taken from experiment. In Sec. III we present results for both the Bobetic-Barker potential and the Dymond-Alder potential using the lowest-order self-consistent phonon scheme.[10] Anticipating our results, we will see that these calculations rule out the Dymond-Alder potential as it gives both a poor ground-state energy and phonon spectrum. In some respects the calculation of Secs. II and III can be regarded as the systematics necessary before investigating a more sophisticated self-consistent phonon theory. Finally, in Sec. IV we discuss the possibility of extracting information about the pair potential and possible three-body forces from experiments on the solid.

II. LATTICE DYNAMICS OF ^{36}Ar WITH BOBETIC-BARKER POTENTIAL AND THREE-BODY FORCES

The dynamical matrix derivable from the potential energy given in Eq. (3) within the quasiharmonic approximation is discussed in detail in Ref. 1. In this paper we shall be primarily concerned with the one-phonon inelastic-scattering cross section. This, following Baym,[11] is proportional to the imaginary part of the thermodynamic Green's function for the phonon, namely,

$$\frac{2\omega(qj)\Gamma(qj,\Omega)}{[\omega(qj)^2-\Omega^2+2\omega(qj)\Delta(qj,\Omega)]^2+4\omega(qj)^2\Gamma(qj,\Omega)^2}\,. \tag{4}$$

Using quasiharmonic frequencies $\omega(qj)$ as a basis, the lowest-order perturbation-theory contributions to $\Delta(qj,\Omega)$ and $\Gamma(qj,\Omega)$ are given by[12]

$$\Delta(qj,\Omega)=-\frac{18}{\hbar^2}\sum_{q_1q_2j_1j_2}\left|V\begin{pmatrix}q & q_1 & q_2\\ j & j_1 & j_2\end{pmatrix}\right|^2 F(\Omega)$$
$$+\frac{12}{\hbar}\sum_{q_1j_1}V\begin{pmatrix}q & -q & q_1 & -q_1\\ j & j & j_1 & j_1\end{pmatrix}(2n_1+1)\,, \tag{5}$$

$$\Gamma(qj,\Omega)=\frac{18\pi}{\hbar^2}\sum_{q_1q_2j_1j_2}\left|V\begin{pmatrix}q & q_1 & q_2\\ j & j_1 & j_2\end{pmatrix}\right|^2 G(\Omega)\,, \tag{6}$$

where $n_1=n(q_1j_1)$ is the population factor of the mode $\omega_1=\omega(q_1j_1)$,

$$F(\Omega)=\left(\frac{n_1+n_2+1}{(\omega_1+\omega_2+\Omega)_p}+\frac{n_1+n_2+1}{(\omega_1+\omega_2-\Omega)_p}\right.$$
$$\left.+\frac{n_1-n_2}{(\omega_1-\omega_2+\Omega)_p}+\frac{n_2-n_1}{(\omega_1-\omega_2-\Omega)_p}\right) \tag{7}$$

and

$$G(\Omega)=(n_1+n_2+1)[\delta(\omega_1+\omega_2-\Omega)-\delta(\omega_1+\omega_2+\Omega)]$$
$$+(n_2-n_1)[\delta(\omega_1-\omega_2-\Omega)-\delta(\omega_1-\omega_2+\Omega)]\,. \tag{8}$$

The anharmonic coefficients

$$V\begin{pmatrix}q & \cdots\\ j & \cdots\end{pmatrix},$$

are essentially Fourier transforms of the cubic and quartic terms in the expansion of the potential energy [Eq. (3)] in powers of the displacements.[3]

In our calculations the quasiharmonic basis frequencies were obtained from force constants that included explicitly the three-body Axilrod-Teller force. The method of calculation is described in detail by Bobetic and Barker.[1] We stress that in order for the three-body terms to be included meaningfully in the dynamical matrix at least nine sets of neighbors must be included. For the two-body force, 42 shells of neighbors were included. The contribution of the three-body force to the basis frequencies is rather small, as was noted previously by Götze and Schmidt.[13] In particular, the shear modes appear to be unaffected by the three-body forces [Eq. (2)] and the longitudinal modes increase by less than about 4% (see Table I for typical examples). In calculating the anharmonic force constants that appear in Eqs. (5) and (6), we have included four shells of neighbors and only the derivatives of the pair potential [Eq. (1)]. The following representation of principal values and δ functions occurring in Eqs. (7) and (8) was adopted, with the choice of ϵ being dictated by the

TABLE I. Selected phonon frequencies (in THz) for ^{36}Ar calculated using Eqs. (1)–(9); ω is the quasiharmonic frequency and Ω the renormalized frequency identified as the peak in Eq. (4). Values in parentheses are calculated with $\nu = 0$ in Eq. (2).

Mode	$T = 4$ °K, $a = 5.315$ Å		$T = 40$ °K, $a = 5.350$ Å		$T = 77$ °K, $a = 5.445$ Å	
	ω	Ω	ω	Ω	ω	Ω
(0.1, 0, 0)L	0.287(0.276)	0.301(0.290)	0.266(0.255)	0.286(0.275)	0.211(0.199)	0.253(0.243)
(0.7, 0, 0)L	1.75 (1.72)	1.83 (1.80)	1.64 (1.61)	1.75 (1.73)	1.34 (1.31)	1.57 (1.54)
(0.1, 0.1, 0)L	0.465(0.451)	0.486(0.473)	0.431(0.417)	0.461(0.448)	0.346(0.332)	0.413(0.401)
(0.1, 0.1, 0)T_1	0.304(0.304)	0.314(0.314)	0.285(0.285)	0.292(0.292)	0.239(0.238)	0.250(0.250)
(0.1, 0.1, 0)T_2	0.194(0.195)	0.199(0.199)	0.183(0.184)	0.185(0.186)	0.156(0.157)	0.160(0.161)
(0.1, 0, 0)T	0.215(0.215)	0.222(0.222)	0.202(0.201)	0.206(0.206)	0.169(0.169)	0.175(0.174)
(0.7, 0, 0)T	1.22 (1.22)	1.27 (1.27)	1.15 (1.14)	1.23 (1.23)	0.958(0.957)	1.13 (1.12)

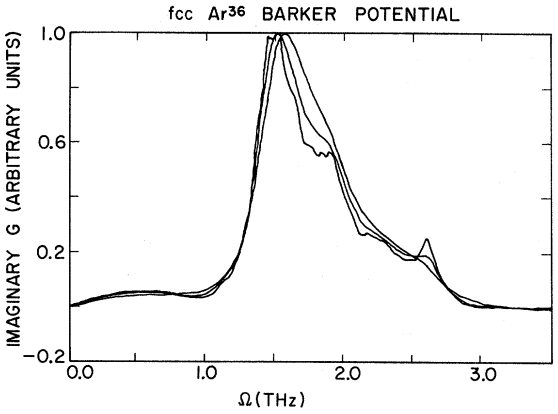

FIG. 2. Imaginary part of the Green's function [Eq. (4)] for the L phonon (0.7, 0, 0) in ^{36}Ar at 77 °K and $a = 5.445$ Å. The various curves show the sensitivity of ImG to the representation of the principal value and δ function.

grid size used in the Brillouin-zone (BZ) sums:

$$\pi\delta(x) = \frac{\epsilon}{x^2+\epsilon^2}\,, \quad \frac{1}{(x)_p} = \frac{x}{x^2+\epsilon^2}\,. \tag{9}$$

The difficulties associated with this procedure have been discussed in the literature[12,14,15] and ways of circumventing the difficulties have been proposed.[16] Figure 2 shows one of the extreme examples of the sensitivity of Eq. (4) to the choice of ϵ. The smaller the value of ϵ for a given grid size (in this case 259 points in $\frac{1}{48}$ of the BZ), the greater the fine structure that appears in Eq. (4). There is thus some ambiguity in the appropriate value of ϵ. However, for most phonons examined in this paper this has less than a 1% effect on the position of the peak. Figure 3 shows a breakdown of the various contributions to Eq. (4) for the transverse phonon (0.7, 0, 0) at 40 °K with lattice constant $a = 5.35$ Å. $\Delta(\Omega)$ and $\Gamma(\Omega)$ can be identified readily in Fig. 3 since $\Gamma(0) = 0$ and $\Delta(0) \neq 0$; also $\times$ indicates the quasiharmonic frequency ω and + indicates $\omega + \Delta(\omega)$. The third curve in Fig. 3 shows the imaginary part of the Green's function for this phonon, i.e., Eq. (4).

Using the procedures outlined above, we have made a detailed study of the temperature dependence of phonons in fcc ^{36}Ar under the conditions of the experiment of Batchelder, Haywood, and Saunderson.[9] Selected phonon energies are given in Table I. Here the peak in the imaginary part of the Green's function [Eq. (4)] is identified as the renormalized frequency Ω. Figs. 4–9 show plots of Eq. (4) for various phonons propagating along the [ξ 0 0] direction as a function of temperature. Certain systematics appear in these calculations. The high-energy L phonons are predicted to be broad at all temperatures. In contrast the T pho-

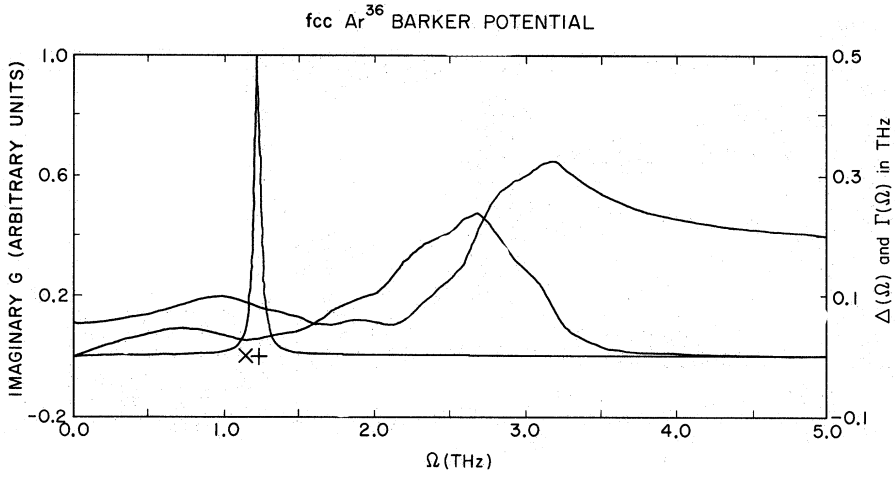

FIG. 3. The sharply peaked curve is the imaginary part of the Green's function [Eq. (4)] for the T phonon (0.7, 0, 0) in ^{36}Ar at 40 °K and $a = 5.35$ Å. Also shown is $\Delta(\Omega)$ [Eq. (5)] and $\Gamma(\Omega)$ [Eq. (6)] which are readily identified since $\Delta(0) \neq 0$ and $\Gamma(0) = 0$. The quasiharmonic frequency ω is indicated by an × and $\omega + \Delta(\omega)$ is shown as a +.

nons at 77 °K appear to be little broader than the corresponding L phonons at 4 °K. When one recalls that the plots in Figs. 4–9 have been arbitrarily normalized to unit peak height, one anticipates, on the basis of these calculations, great difficulty in detecting high-energy longitudinal phonons at high temperatures. Since the three-body force [Eq. (3)] makes very little contribution to T phonon energies for the [ξ 0 0] direction, this phonon branch should be particularly sensitive to the pair potential.

A detailed comparison is made with the data of Batchelder, Haywood, and Saunderson[9] in Table II and in Figs. 10 and 11. Superficially at both 4 and 40 °K there appears to be a rather good fit to the experimental data (cf. Table II). However, the calculated shift $[\Omega(40\,^\circ\mathrm{K}) - \Omega(4\,^\circ\mathrm{K})]/[\Omega(4\,^\circ\mathrm{K})]$ shown in Fig. 10 is much too small and incidentally fitted rather well by a solely quasiharmonic shift! The situation at 77 °K, illustrated in Fig. 11, is much the same. The disagreement at 77 °K is not too disturbing because at those high temperatures the simple quasiharmonic perturbation approach used in this paper is known to have deficiencies, but at 40 °K and using the observed lattice constant this should not be the case. In fact, one might then be tempted to blame the potential for this disagreement. However, a calculation[17] using a very different potential, namely, a nearest-neighbor (12-6) Lennard-Jones potential, gave results for the temperature shifts very similar to those presented here. This latter calculation employed self-consistent phonon theory and so is not strictly comparable to the present work, although it is a little surprising that such rather different calculations agreed with each other and were so different from experiment. Before rejecting the Bobetic-Barker potential, a more careful examination of the high-temperature calculations, using, for example, a self-consistent phonon theory,[10]

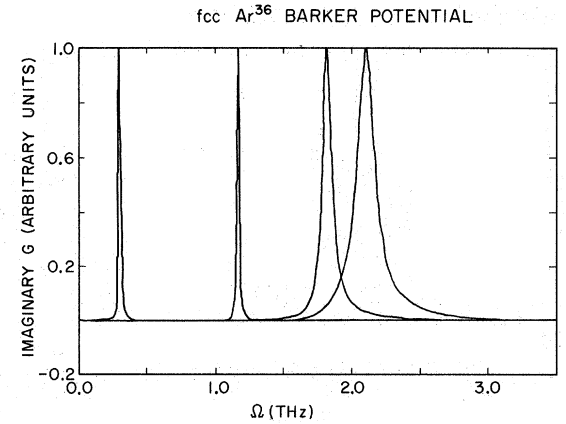

FIG. 4. Imaginary part of the Green's function [Eq. (4)] for L phonons propagating in the [ξ00] direction (ξ = 0.1, 0.4, 0.7, 1.0) of ^{36}Ar at 4 °K and $a = 5.315$ Å.

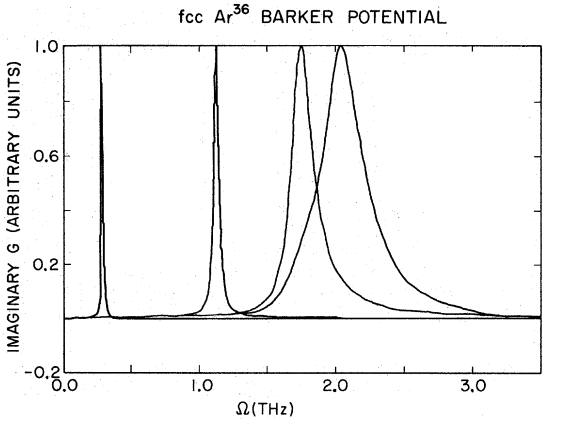

FIG. 5. Imaginary part of the Green's function [Eq. (4)] for L phonons propagating in the [ξ00] direction (ξ = 0.1, 0.4, 0.7, 1.0) of ^{36}Ar at 40 °K and $a = 5.350$ Å.

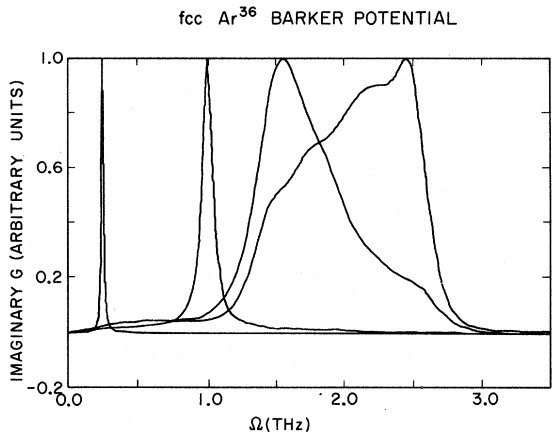

FIG. 6. Imaginary part of the Green's function [Eq. (4)] for L phonons propagating in the [ξ00] direction (ξ=0.1, 0.4, 0.7, 1.0) of ^{36}Ar at 77 °K and a=5.445 Å.

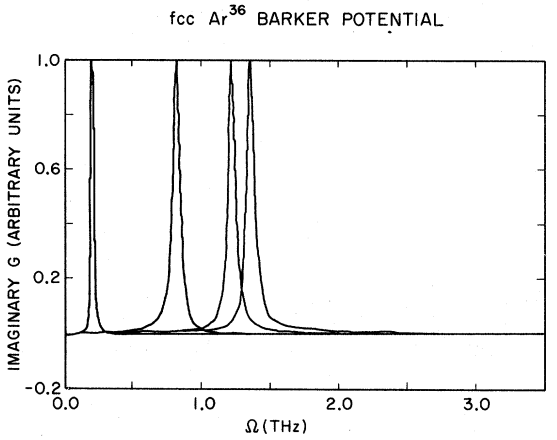

FIG. 8. Imaginary part of the Green's function [Eq. (4)] for T phonons propagating in the [ξ00] direction (ξ=0.1, 0.4, 0.7, 1.0) of ^{36}Ar at 40 °K and a=5.350 Å.

must be undertaken. With these facts in mind we examine in Sec. III both a radically different interatomic potential and the lowest-order self-consistent phonon theory.

III. SELF-CONSISTENT PHONON THEORY WITH BOBETIC-BARKER AND DYMOND-ALDER POTENTIALS

The lowest-order self-consistent phonon theory is most easily derived from a variational approach to the free energy.[18] In summary, at zero temperature, the ground-state energy of a system interacting with pair potentials is given by

$$E=\frac{1}{2}\sum_{i,j}\langle\phi^{(2)}(R_{ij}+u_i-u_j)\rangle_s+\frac{1}{4}\sum_{qj}\hbar\omega_{qj}\,, \qquad (10)$$

where ω_{qj} are frequencies that are to be obtained from a dynamical matrix whose force constants are given by[18]

$$\Phi_{ij}=\langle\nabla\nabla\phi^{(2)}(R_{ij}+u_i-u_j)\rangle_s\,. \qquad (11)$$

Here $\langle\,\rangle_s$ denotes an average to be taken with respect to the displacement-displacement correlation function, which itself depends upon the frequencies ω_{qj} and hence the self-consistency.

We have evaluated the ground-state energy and the frequencies ω_{qj} for the Bobetic-Barker potential [Eq. (1)] and the Dymond-Alder potential. The phonons are shown in Fig. 12, where they are compared with experimental data taken at liquid He temperatures.[9,19,20] The ground-state energy is given in Table III, and this too is compared with experiment.[21] In computing the ground-state energy for the Bobetic-Barker potential, the three-body force [Eq. (3)] was added without averaging it self-consistently. The contribution of the three-body force to the dynamical matric was incorporated in a similar fashion.

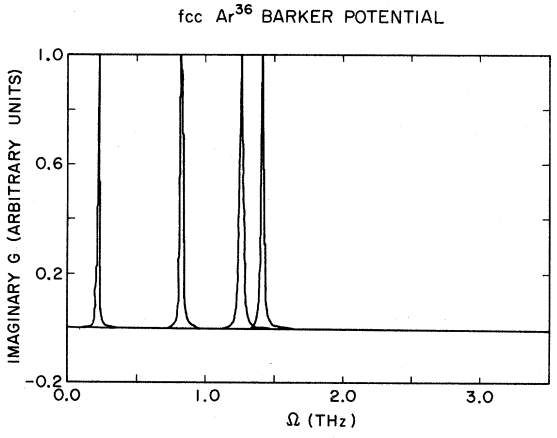

FIG. 7. Imaginary part of the Green's function [Eq. (4)] for T phonons propagating in the [ξ00] direction (ξ=0.1, 0.4, 0.7, 1.0) of ^{36}Ar at 4 °K and a=5.315 Å.

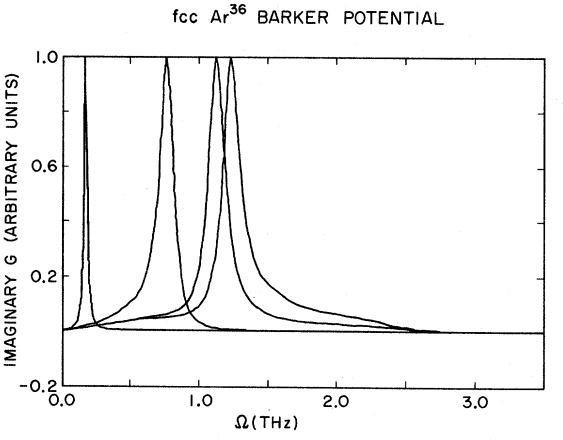

FIG. 9. Imaginary part of the Green's function [Eq. (4)] for T phonons propagating in the [ξ00] direction (ξ=0.1, 0.4, 0.7, 1.0) of ^{36}Ar at 77 °K and a=5.445 Å.

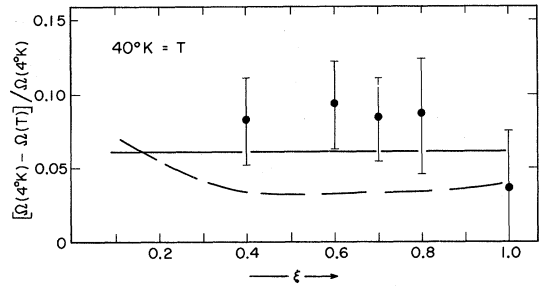

FIG. 10. Relative frequency shifts for T phonons in the [ξ00] direction of ^{36}Ar. The experimental points $[\Omega(4\,^{\circ}\mathrm{K}) - \Omega(T)]/\Omega(4\,^{\circ}\mathrm{K})$ are taken from Ref. 9. The solid line is the quasiharmonic shift, the dashed line is calculated as described in the text.

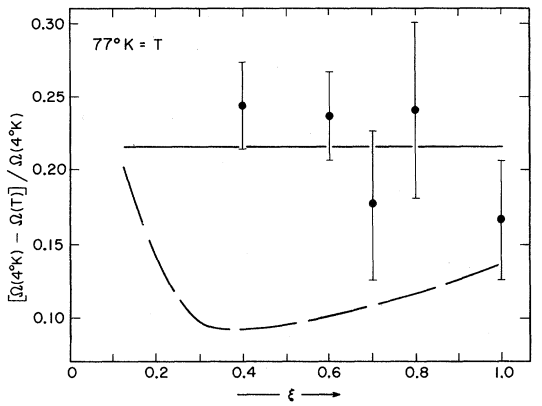

FIG. 11. Relative frequency shifts for T phonons in the [ξ00] direction of ^{36}Ar. The experimental points $[\Omega(4\,^{\circ}\mathrm{K}) - \Omega(T)]/\Omega(4\,^{\circ}\mathrm{K})$ are taken from Ref. 9. The solid line is the quasiharmonic shift, the dashed line is calculated as described in the text.

The Dymond-Alder potential is seen to be incompatible with the experimental phonon data and the ground-state energy. While the Dymond-Alder potential does not violate the bound on the ground-state energy provided by the variational approach, the leading corrections to the ground-state energy are known to be small. In fact, for the Bobetic-Barker potential we have evaluated the three-phonon correction to the ground-state energy (the so called improved self-consistent phonon theory[22]) and find this to be -1.2 cal mole^{-1}. As yet we have not evaluated the corrections to lowest-order self-consistent phonons due to three-phonon and higher-order processes. However, these are known[14,23] to lower the phonon energies and so will rule out the Dymond-Alder potential completely but not the Bobetic-Barker potential.

IV. INTERPRETATION OF PHONON DISPERSION CURVES

In Sec. III we saw that the experimental phonon data and the ground-state energy completely ruled out the Dymond-Alder potential but not the Bobetic-Barker potential. In this section we wish to examine to what extent measured phonon curves can give us information about the forces in the solid. To do this we calculated phonons at 0 °K for the Bobetic-Barker potential for the symmetry directions [ξ 0 0], [ξ ξ 0], and [ξ ξ ξ]. These phonon energies (140 in all) included the three-body force equation (3) that was summed over nine neighbors and also allowance was made for vibrational anharmonicity.[2] These latter two effects, when they contributed, were at about the 5% level. These phonons were then regarded as experimental data and a force-constant analysis was undertaken in an attempt to extract the input information on the forces.

An unweighted least-squares fit of the 140 phonons to (i) a general tensor (GT) force model for first through fourth neighbors (which is as far as one can go with the symmetry direction data) and (ii) an axially-symmetric (AS) force-model fit for first through eighth neighbors. The GT model agreed extremely closely with the AS model, i.e., the model parameters obeyed the conditions of axial symmetry to better than 0.2%, even though these conditions were not imposed in the GT fit. The fifth-neighbor AS model seemed to fit the data perfectly but in the light of presently available experimental accuracy the third-neighbor AS model provided an excellent fit. This latter model almost obeyed the equilibrium condition for central forces, although this constraint was not imposed and certainly not included in the primary data. It therefore appears to us unlikely at present that phonon data will yield definitive information on the non-

TABLE II. Selected phonon frequencies (in THz) observed and calculated using Eqs. (1)–(9) for transverse modes in ^{36}Ar for the [ξ00] direction. The theoretical inverse lifetime Γ is shown in parenthesis.

	$T=4$ °K, $a=5.315$ Å		$T=40$ °K, $a=5.350$ Å		$T=77$ °K, $a=5.445$ Å	
ξ	ν(calc)	ν(obs)	ν(calc)	ν(obs)	ν(calc)	ν(obs)
0.4	0.84(0.002)	0.89 ± 0.03	0.81(0.03)	0.82 ± 0.03	0.76(0.08)	0.68 ± 0.03
0.7	1.27(0.006)	1.32 ± 0.03	1.23(0.03)	1.21 ± 0.03	1.13(0.08)	1.09 ± 0.07
1.0	1.43(0.008)	1.40 ± 0.03	1.37(0.03)	1.35 ± 0.04	1.23(0.08)	1.17 ± 0.04

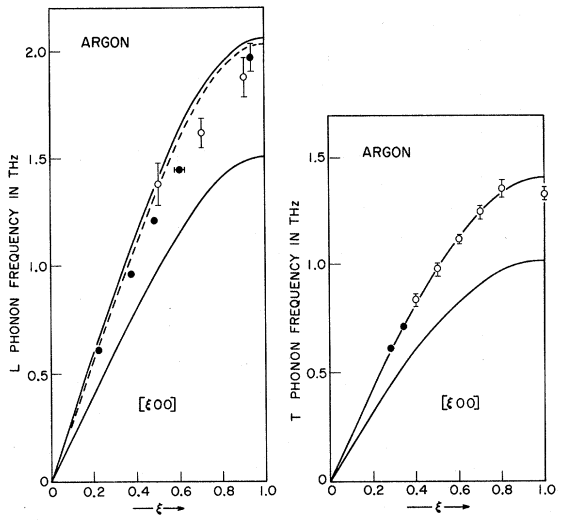

FIG. 12. Phonons for [ξ00] direction in Ar. The open circles are taken from Ref. 9 scaled by $\frac{49}{36}$. The solid circles are from Refs. 19 and 20. The upper solid (dashed) curve is a self-consistant phonon calculation for the Bobetic-Barker potential with (without) three-body forces. The lower solid curve is a self-consistent phonon calculation for the Dymond-Adler potential (see text).

additivity of interatomic forces in solid Ar. In this regard the best hope would seem to lie with studies of the phonons of long wavelength by Brillouin-scattering techniques.[24,25] These experiments determine the elastic constants which seem to be most sensitive to three-body forces.[2] On the other hand, as we have seen in Secs. II and IV, the phonon energies and their temperature dependence seem to provide a very stringent test of the dynamical model and the pair potential.

V. CONCLUSION

We have used pair potentials for Ar atoms derived from gas-phase properties to calculate phonon energies for the solid. The low-temperature phonon data appear to rule out an interatomic potential proposed by Dymond and Alder[6] but not that of Bobetic and Barker.[1] The latter potential has been used to calculate the temperature dependence of phonons propagating along [ξ 0 0]. The temperature dependence of the T branch was in poor agreement with the experimental data of Batchelder, Haywood, and Saunderson.[9] The reasons for the disagreement are not understood but may be due to inadequacies in either the pair potential or the dynamical model. From a force-constant analysis of theoretical phonon curves, we conclude that it will be difficult to extract information about three-body forces in solid Ar from measured phonon curves with presently available accuracy. In this regard, there appears to be an urgent need for Brillouin-scattering experimental solid Ar to complement the neutron scattering data.

TABLE III. Ground-state energy of solid Ar in cal mole^{-1}.

	Without three-body force	With three-body force
Barker-Bobetic	−1981	−1844
Dymond-Alder	−1807	
Expt (Ref. 21)	−1846 ±7	

Finally, we mention that Doran and Zucker[26] and Hüller[27] have studied the higher-order nonadditive multipole forces. Individually, in magnitude, these were found to be as large as 20% of the triple-dipole force in Eq. (2). However, through a fortuitous cancellation,[26] these higher-order terms give completely negligible contributions to the solid-state properties of Ar. Thus any inadequacy in our choice of potential-energy function for the solid [i.e., Eq. (3)] will probably reflect the importance of nonadditive exchange forces which have been omitted completely in our work.[28]

ACKNOWLEDGMENTS

We would like to thank Dr. Gerald Dolling of AECL, Chalk River, Ontario, for carrying out the fitting procedure described in Sec. IV and Dr. D. N. Batchelder and Dr. D. H. Saunderson for sending us details of their work prior to publication.

*Issued as National Research Council of Canada Report No. 12011 (unpublished).

[1]M. V. Bobetic and J. A. Barker, Phys. Rev. B 2, 4169 (1970).

[2]J. A. Barker, M. L. Klein, and M. V. Bobetic, Phys. Rev. B 2, 4176 (1970).

[3]J. A. Barker and A. Pompe, Australian J. Chem. 21, 1683 (1968).

[4]B. M. Axilrod, J. Chem. Phys. 17, 1349 (1949).

[5]J. A. Barker, D. Henderson, and W. R. Smith, Mol. Phys. 17, 579 (1969).

[6]J. H. Dymond and B. J. Alder, J. Chem. Phys. 51, 309 (1969).

[7]J. A. Barker, M. V. Bobetic, and A. Pompe, Mol. Phys. 20, 347 (1971).

[8]L. Bruch and I. J. McGee, J. Chem. Phys. 53, 4711 (1970).

[9]D. N. Batchelder, B. C. G. Haywood, and D. H. Saunderson, J. Appl. Phys. 41, 5091 (1970); J. Phys. C (to be published).

[10]T. R. Koehler, Phys. Rev. Letters 17, 89 (1966); V. V. Goldman, G. K. Horton, and M. L. Klein, *ibid.* 24, 1424 (1970).

[11]G. Baym, Phys. Rev. 121, 741 (1961).

[12]R. A. Cowley, Advan. Phys. 12, 421 (1963).

[13]W. Götze and H. Schmidt, Z. Physik 192, 409 (1966).

[14]L. Bohlin and T. Högberg, J. Phys. Chem. Solids 29, 1805 (1968).
[15]A. A. Maradudin, A. E. Fein, and G. H. Vineyard, Phys. Status Solidi 2, 1479 (1962).
[16]V. V. Goldman, G. K. Horton, T. Keil, and M. L. Klein, J. Phys. C 3, 133 (1970).
[17]G. K. Horton, V. V. Goldman, and M. L. Klein, J. Appl. Phys. 41, 5139 (1970).
[18]N. S. Gillis, N. R. Werthamer, and T.R. Koehler, Phys. Rev. 165, 951 (1968).
[19]H. Egger, M. Gsänger, and E. Lüscher, Phys. Letters 28A, 433 (1968).
[20]B. Dorner and H. Egger. Phys. Status Solidi 43, 611 (1971).
[21]R. H. Beamont, H. Chihara, and J. A. Morrison, Proc. Phys. Soc. (London) 78, 1462 (1961).
[22]V. V. Goldman, G. K. Horton, and M. L. Klein, Phys. Rev. Letters 24, 1424 (1970).
[23]T. R. Koehler, Phys. Rev. Letters 22, 777 (1969).
[24]H. Meixner, G. Winterling, W. Heinicke, and M. Gsänger, Phys. Letters 31A, 295 (1970).
[25]W. S. Gornall and B. P. Stoicheff, Solid State Commun. 8, 1529 (1970).
[26]M. B. Doran and I. J. Zucker, J. Phys. C 4, 307 (1971).
[27]A. Hüller (unpublished).
[28]C. E. Swenberg, Phys. Letters 24A, 163 (1967).

PHYSICAL REVIEW B VOLUME 4, NUMBER 6 15 SEPTEMBER 1971

Infrared Absorption of U Centers in CsBr and CsI†

C. G. Olson and D. W. Lynch
Institute for Atomic Research and Department of Physics, Iowa State University, Ames, Iowa 50010
(Received 30 April 1971)

Measurements were made of the absorption of the infrared-active local mode of H^- and D^- substitutional impurities in CsBr and CsI from 5 to about 100 K. In CsBr, the T^2 dependence of the half-width above about 30 K indicates the local mode is broadened by the Raman or scattering mechanism, while the constant low-temperature half-widths are characteristic of the decay of the local mode into three (D^-) or four (H^-) lattice phonons. The sidebands are weak, and are described well by the model of Bilz, Fritz, and Strauch, in which the polarizability of the impurity is important. The resultant lattice density of states for CsBr is in good agreement with that calculated by Karo and Hardy using a model with the deformation dipoles on anions only. The main absorption peak in CsI was not Lorentzian, but no origin for the unresolved structure was found. The phonon density of states deduced from the sidebands in CsI agrees reasonably well with Karo and Hardy's calculated curve.

INTRODUCTION

A U center is a hydrogen or deuterium negative ion at a normal cation site in an alkali or alkaline-earth halide. The very light mass of this ion results in a threefold degenerate vibrational mode which cannot propagate through the lattice, a mode which is confined to the immediate vicinity of the defect. The excitation of this localized mode gives rise to a narrow temperature-dependent infrared absorption peak.[1] In addition, the defect destroys the translational invariance of the crystal, removing the wave-vector selection rule for optical processes. The result is the occurrence of sidebands on the main local-mode absorption peak, corresponding to the excitation of the local mode plus the creation or absorption of a lattice phonon.

Measurements of the peak position of the local-mode absorption and its dependence on the mass of the defect (isotope effect) give information on the force-constant changes which occur when the defect is introduced. Measurements of the half-width of the local-mode peak as a function of temperature, and its isotope effect, yield information on the anharmonic coupling of the local mode to the lattice, and on the decay mechanism of the excited local mode. The observed sidebands can be compared with the density of states for the phonons in the perfect crystal or, if necessary, in the crystal with defects. The temperature dependence of the peak position can be observed, but its interpretation is not clear.

Studies of the U center local mode have been carried out for most alkali halides of the NaCl structure,[1-5] and a very complete study[6] was made for alkaline-earth fluorides. Very little work has been reported for U centers in the CsCl lattice, the only work[7-10] being at temperatures above 20 K. The isotope effect was not studied completely, nor was the low-temperature limit of the width of the main peak. Sidebands were found on the CsCl and CsBr local-mode peak,[10] but not CsI, and the resolution was limited. The sidebands are important because the phonon spectrum for the cesium halides has never been measured by inelastic neutron scattering. Our sideband measurements on CsBr strongly favor one of four calculated spectra based on different force-constant models. We also are able to analyze the shape of the main peak in CsBr. Our data on CsI are difficult to inter-